

Launch Dynamics Environment of a Water Piercing Missile Launcher

Jon J. Yagla

DTI Associates, Dahlgren, VA

John Busic, Samuel Koski, Brian Myruski

NSWC Dahlgren Division, Engagement Systems Department, Dahlgren, VA

Chris Weiland and Pavlos Vlachos

Virginia Tech College of Engineering, Blacksburg, VA

INTRODUCTION

The Water Piercing Missile Launcher (WPML) is based on the Concentric Canister Launcher (CCL). The launcher uses the gas jet emitted from the CCL to pierce the ambient water above a submarine or other submerged platform. The missile is then released and flies through the gas column to the surface. The launcher has the potential to eliminate pyrotechnic gas generators and pumps as the means of expelling missiles from submarines, and also has the potential for eliminating complex and noisy pressure balancing systems. Each WPML is a complete launching system, which houses the missile during transport, guides the missile during its initial flight, provides self-contained gas management, and contains all of the necessary electronics to launch a missile [1]. Costs may also be reduced as compared to existing systems that employ pyrotechnic gas generators and complex pressure balancing systems.

The CCL is composed of two concentric tubes joined by longerons running the length of the tubes and spaced at 90-degree intervals, Figure 1. The longerons provide structural support for the CCL. The missile is housed in the inner cylinder. The rocket motor nozzle end of the launcher is capped by a hemisphere, with a radius equal to the outer cylinder radius. Thrust augmentation (gun effect) is controlled by a port near the motor nozzle exit. Exhaust gases from the rocket motor strike the hemispherical end-cap and are re-routed 180-degrees through the annular region between the two cylinders, exiting at the tip of the launcher. Thus, the exhaust gases are safely re-directed along the line of fire, Figure 2.



Figure 1. Concentric Canister Launcher

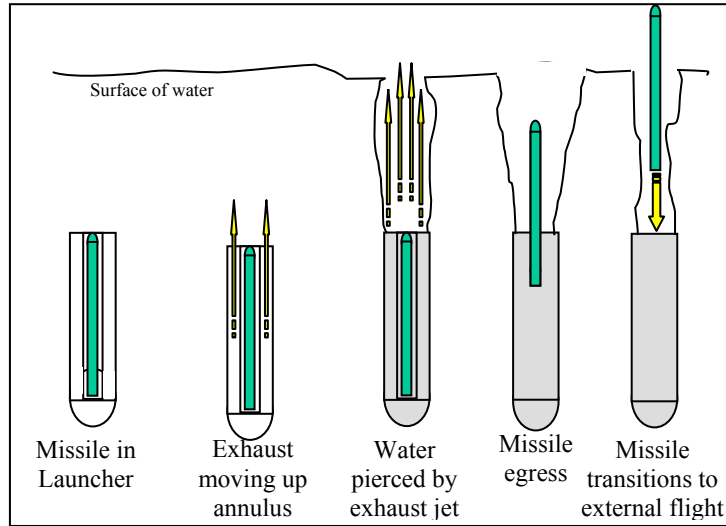


Figure 2. Water Piercing Missile Launcher Concept.

A two-dimensional Navier-Stokes calculation was performed to simulate the effects of 21-inch diameter booster motor inside a submerged CCL. The computer code used was CFDLIB, which was developed by Los Alamos National Laboratory. The water is represented as Lagrangian mass points, related to each other through stress-strain constitutive equations. The stress in the fluid is caused by relative motion of individual particles. An inflow boundary condition of rocket-motor exhaust was located at the exit plane of the CCL. The boundary condition at the exit was calculated using an in-house semi-empirical code called LAX. Figure 3 shows the volume fraction contours for three different time steps using CFDLIB. Superimposed on the contours is an uncoupled rigid-body dynamics solution of a cruise missile exiting the CCL and flying through the missile exhaust. The color fringes are blue for water, red for exhaust gas, and intermediate colors for a mixture of gas and water.

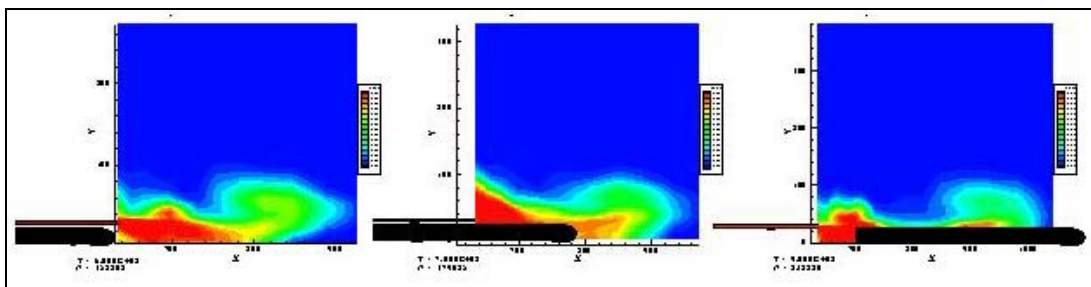


Figure 3. Computer Simulation of Water Piercing Effect and Motion of Missile

Sub scale launchers were built and tested in aquariums. A missile propelled by a 2.75-inch rocket motor was launched and recovered dry from a submerged CCL, Figure 4. Following the favorable result with the 2.75-inch rocket motor, the scale was then doubled and an ~ 8' long x 300 lb. missile propelled by a 5" JATO motor was launched with 20' of water over the launcher, Figures 5 and 6. The figure on the right is a composite view using video camera data for the top half and underwater video for the bottom. The two flashes in the bottom are pyrotechnics fired to release the missile at the right time for it to arrive at the surface at exactly the same time as the jet tip.



Figure 4. Flight Of A Missile Propelled By A 2.75 MK66 Rocket Motor (The Bright Spot On The Left, Over The Tank, Is The Exhaust).



Figure 5. 5-Inch Diameter, 8- Foot Long Missile Propelled By A MK117 JATO Motor.

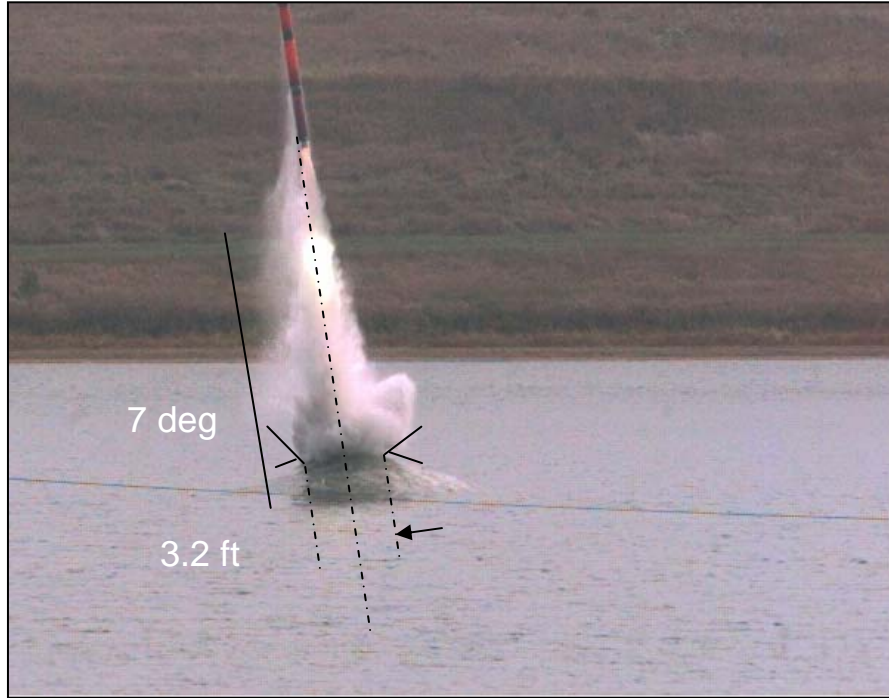


Figure 6. Details The 5-Inch Diameter Missile Transition To Atmospheric Flight.

The remainder of the paper discusses the jet motion and the underwater launch environment. There is very little literature on the formation and initial propagation of transient gas jets in water. Practically all of the literature is about steady jets. Further, there is ample information about water jets in water, and some information about gas jets in air, but very little about gas jets in water.

JET MOTION

The space – time trajectories of the jet tip have been measured for many WPMLs of sizes ranging from 1” to 27” in diameter [2]. The trajectories approximately obey a scaling law, Figure 7. Here the nondimensional jet tip height above the launcher exit plane is plotted against nondimensional time. The jet tip height is nondimensionalized by dividing the observed height by the jet momentum length, L_m , [3]. The nondimensional time is the observed time divided by L_m/V , where V is the jet velocity at the exit plane.

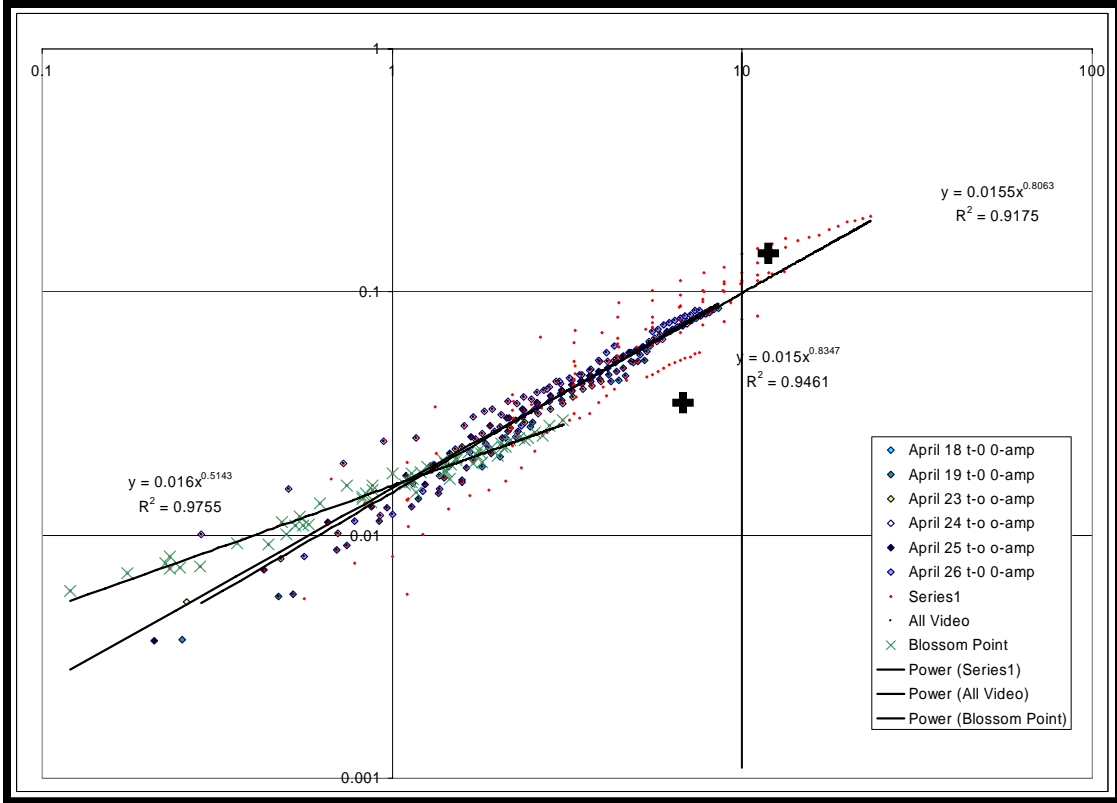


Figure 7. Jet Tip Trajectory Scaled Distance (Ordinate) Versus Scaled Time (Abcissa) Using Data From Mk 66 (2.75-Inch), JATO (5-Inch), And Zuni (5-Inch) Motors At Depths From 6 To 42 Ft. The Mk 66 Motors Were Fired In An 8-Ft Diameter Tank At Blossom Point.

To prepare for the flyout test using the JATO Motor, a preliminary static test with the same launcher was conducted at a depth of 20 ft with only the motor and no missile present. Figure 8 is the space-time trajectory of the JATO at 20 ft depth as determined using an underwater acoustic camera. The formula for the jet tip trajectory is on the upper right corner:

$$y = -6.2508 t^2 + 24.061 t + 0.235 \quad (1)$$

The formula can be differentiated with respect to time to obtain the jet tip velocity:

$$V = -12.5 t + 24.06 \quad (2)$$

These formulae are sufficient to determine the time to release missile in order for it to arrive at the surface at the same time as the jet tip reaches the surface. However they do not provide any details on the internal structure of the jet.

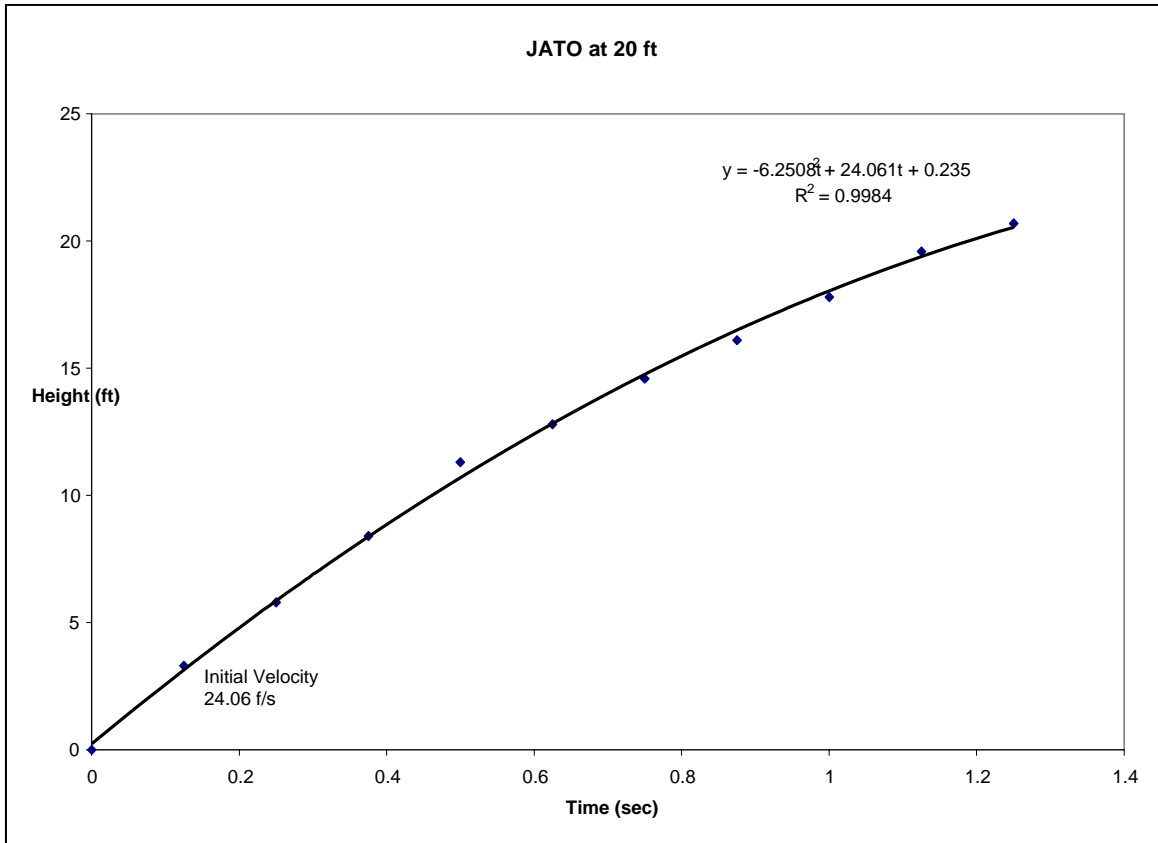


Figure 8. Space-Time Trajectory Of Jet Tip Using JATO Motor And 20 Ft Of Water Over The Launcher.

An assumption that was used to work out the jet flow over the missile is that the jet gas velocity is everywhere the same in the jet and the same as the jet tip: like blowing up a long skinny balloon. There is a high velocity in the filler neck of the balloon, but it fills slowly, so the tip velocity is small by comparison. Equation 2 was used for the jet tip velocity. We consider this a very low order approximation to the launch environment. Better data is now available. However, the launch dynamics were accurately computed with the simple model. There is a considerable effort in the laboratory to refine the launch environment properties using CFD and semi-empirical methods.

JET CHARACTERISTICS

Jet Basics

Figure 9 shows the basic geometry of a steady turbulent round jet [4]. The zone of flow establishment is the region in which the exit geometry is important to the detailed structure of the jet. Beyond this zone the exit geometry doesn't matter, and the profiles of velocity $u(x,r)$ and concentration of entrained materials $c(x,r)$ take

the Gaussian shape as shown in the figure. For the WPML, the outlet is an annulus, so the zone of flow establishment can be determined from the equivalent diameter of the annulus. The equivalent diameter is $(4A/\pi)^{1/2}$, where A is the free area of the annulus. For the JATO launcher the free area is 0.599 sq. ft. and the equivalent diameter is 0.87 ft. Therefore the zone of flow establishment should end 5.4 ft above the launcher.

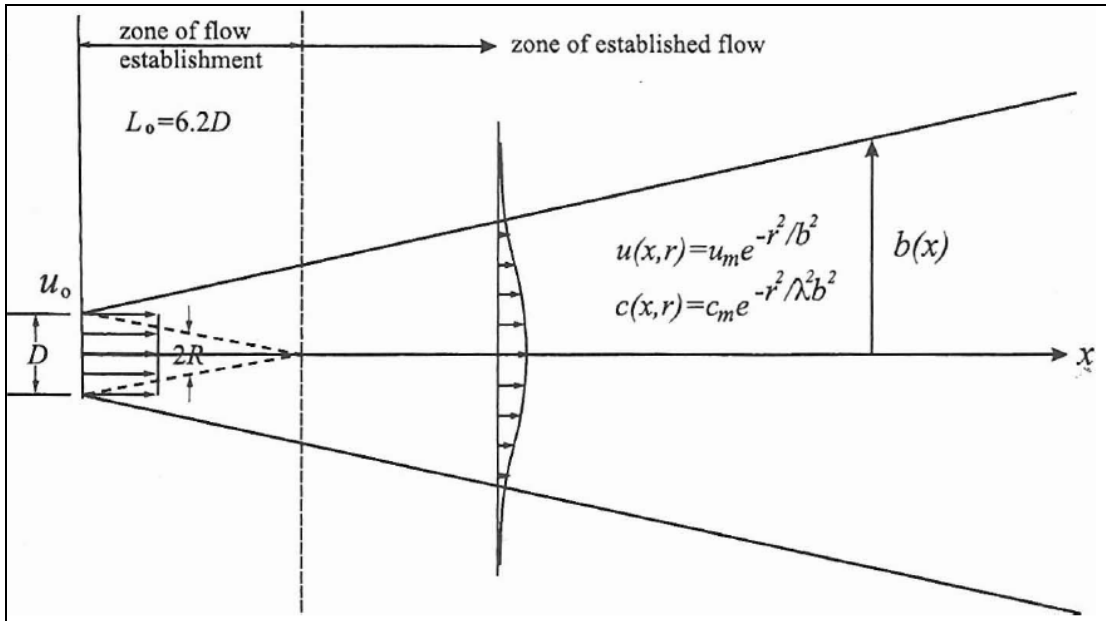


Figure 9. Basic Geometry Of A Turbulent Round Jet.

The data in references 3 and 4 are mainly from water jets discharging into water. For these jets $b(x) = 0.12x$. Here $b(x)$ is the jet radius. The half angle of the cone is 6.8 degrees. For rocket exhaust jets discharging into air, the jets are broader. Figure 10 shows rocket exhaust jets in air for three cases spanning many orders of magnitude in size. The spreading rate is $b(x) = 0.26x$ and the half angle is 13.7 degrees.

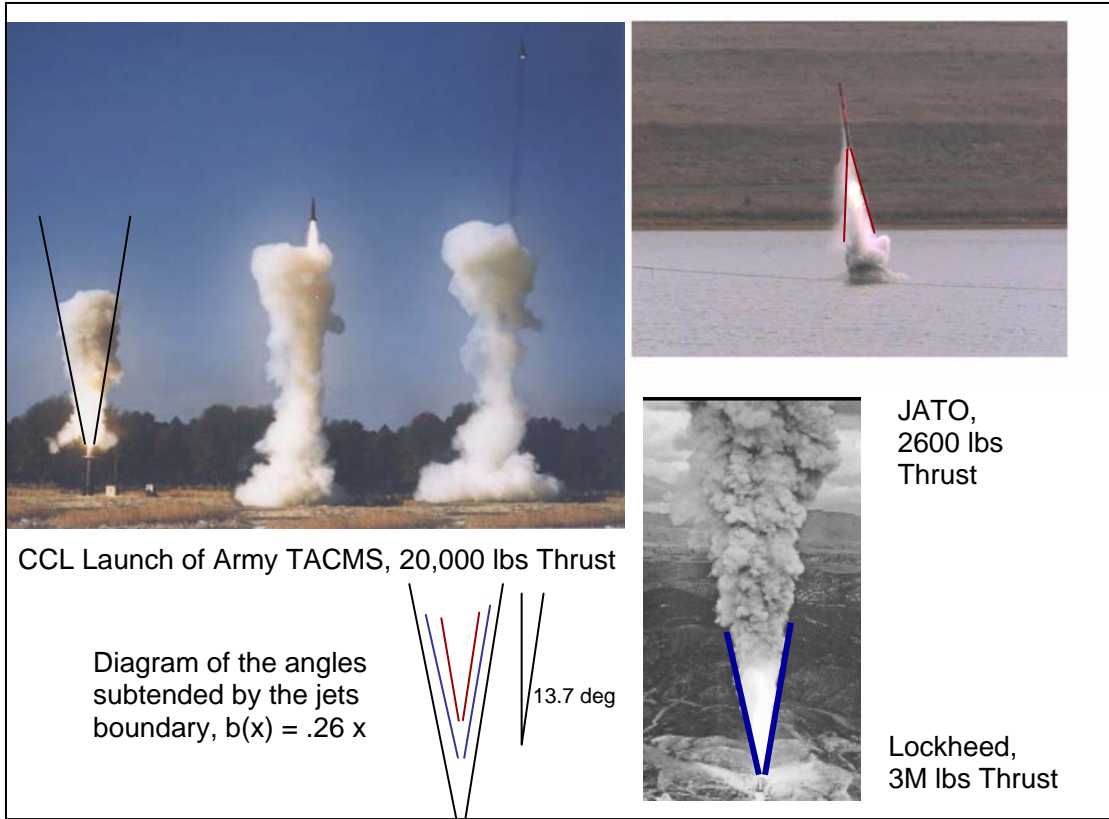


Figure 10. Rocket Exhaust Jets In Air Over A Wide Range Of Motor Sizes.

There is very little data for gas jets discharging into water. Intuition suggests the spreading rate should be insensitive to the exhaust chemical composition and somewhere between the two cases above. A jet from a MK66 motor fired with 10 ft of water over a 7-in diameter CCL is shown in Figure 11. This shows $b(x) = 0.13 x$ and a half angle of 7.4 degrees. The extent to which the cylindrical boundary just four feet from the jet centerline influenced the jet diameter is not known.

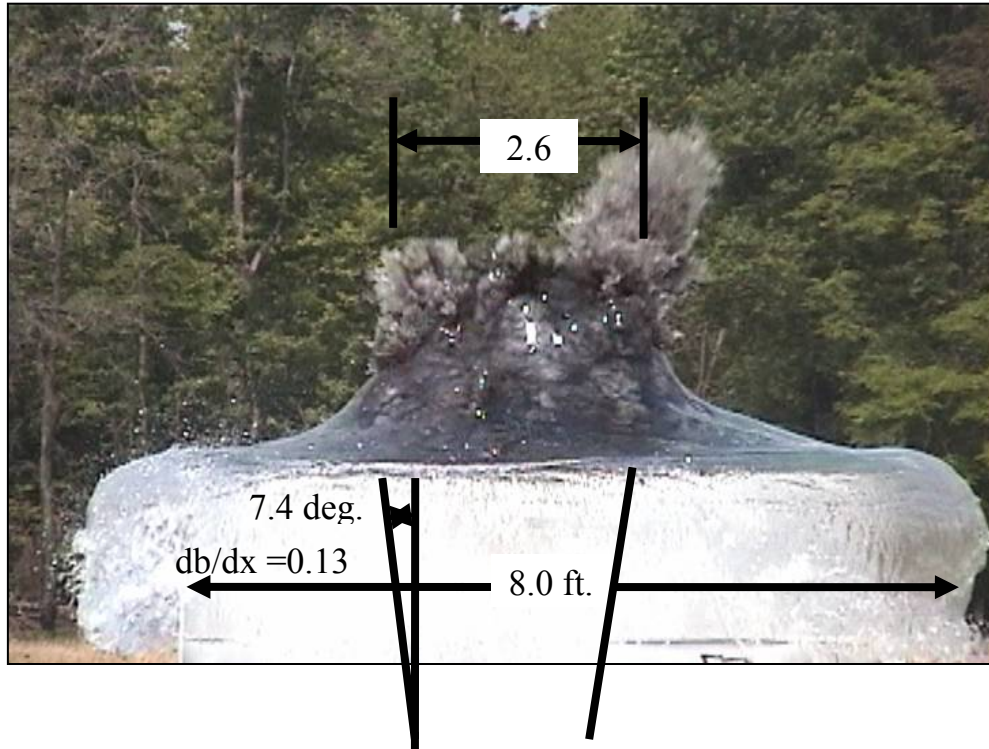


Figure 11. Water Piercing Jet From MK66 Motor At A Depth Of 10 Ft.

The data of Loth and Faeth, [5] for a steady air jet discharging into water show a zone of flow establishment ending at 8 diameters, with a jet width of $.5x$ starting at 8 diameters and diminishing to $.4x$ at 40 diameters, for a broad range of exit conditions from subsonic $M \sim 0.6$ to supersonic with $M > 2$. Their jet width is defined as twice the radius at which the air/water ratio is 0.5. The slope db/dx would be 0.25 decreasing to 0.2. Their data show at $M \sim 0.6$, the centerline of the jet out to 20 diameters is pure air. For $M = 1$ the centerline is pure air out to 30 diameters. As the Mach number was increased, penetration of pure air out to 60 diameters along the centerline was observed. Their data also shows that a region of 90% air at least 4 exit diameters in diameter extends out to 80 diameters for $M = 0.8$ and $M = 1.0$ jets, and even broader and farther for higher Mach numbers. The centerline dynamic pressure is constant at the gas outlet value for 6 diameters, then diminishes very rapidly. The dynamic pressure is down to 10% of the outlet value at 30 diameters. Although greatly diminished, the cross section dynamic pressure profiles are broad enough to affect a missile out to 70 diameters where the diameter of the profile is about 20 exit diameters.

We have been able to obtain sonogram type images, Figure 12, of jets from water piercing missile launchers. They show a nearly constant jet diameter of 0.15 the value of x at the surface. The images show a distinct interface, but the gas/air fraction at the image boundary is not known.

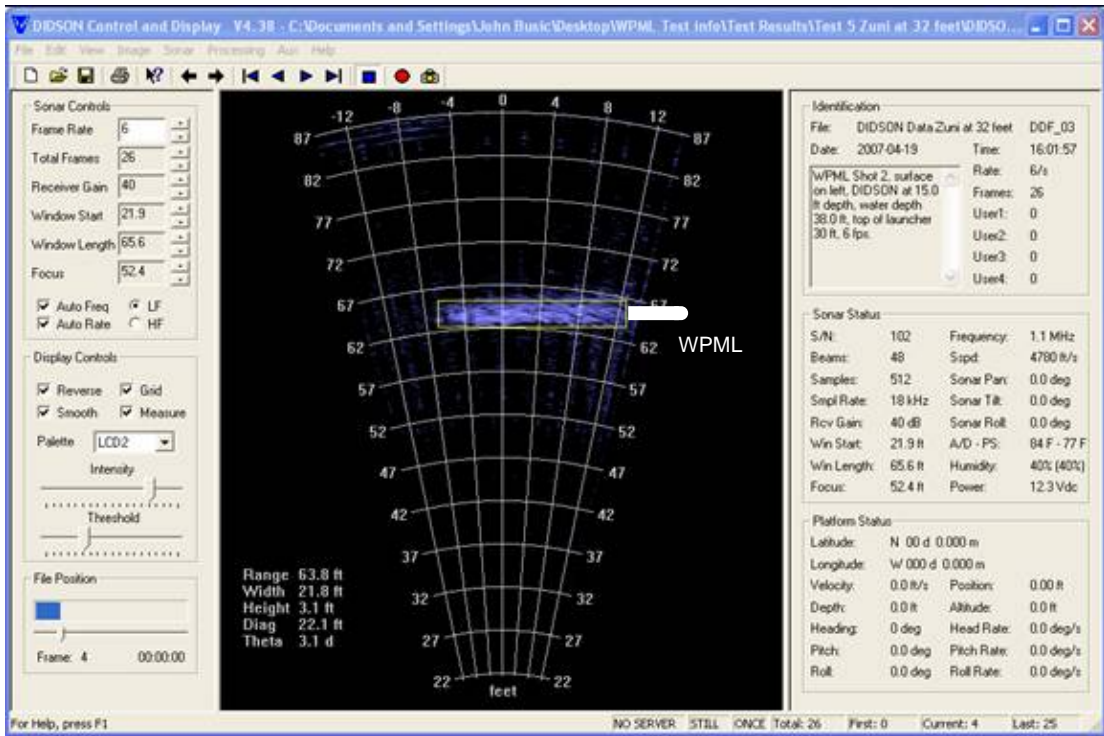


Figure 12. Image Of A Vertical Exhaust Jet From A Water Piercing Missile Launcher From An Acoustic Camera (Rotated 90-Deg, WPML Sketch Added).

LAUNCHER EXIT PLANE PROPERTIES

Computation of the Jet Exit Properties

The jet from a MK117 JATO motor is pure gas as it exits the rocket nozzle and travels up the annular space between the concentric cylinders of the gas management system. The gas properties are computed using the propellant chemical composition and nozzle geometry and an equilibrium thermochemical computer program. The MK 117 JATO motor has properties shown in Table 1. The left side of the table shows the physical properties and the right side shows the thermodynamic state and velocity at the exit. These properties are computed using a one-dimensional CFD program that expands the exhaust into the launcher hemihead and computes wave motion in the annular space. The exit plane ambient pressure depends on the depth over the launcher. The hydrostatic pressure of the water is the exit plane pressure boundary condition for the CFD analysis. This causes the gas to expand to the indicated Mach number. More powerful motors can cause the gas to expand to unity Mach number (choked flow). Notice from the table the sensitivity of the exit condition to the depth.

Table 1. Rocket Exhaust Properties

JATO		
Pressure	psi	1800
Temp	deg K	2377
Mol. Wt.	g-mol	23.23
R	f ² /(s ² R)	2140
Cv	f ² /(s ² R)	9369
Cp	f ² /(s ² R)	11510
Gamma		1.2284

Depth	ft.	10.0	20.0
P	psia	19.1	23.6
V	f/s	1982	1630
Rho	lb/in ³	7.50E-06	9.10E-06
Mach		0.680	0.560

The water provides lateral confinement of the jet, so the spreading rate is less than in air. As the jet moves up and away from the launcher, several processes take place. First is turbulent mixing. The jet has a high Reynold's number and is inherently unstable. Eddies form on the interface between the jet and the water. Water eddies are entrained by the jet, and gas eddies are decelerated and enter the water. This is called turbulent mixing and causes the velocity of the gas to decrease and the entire ambient water medium to be set in motion, with streamlines leading in laterally from afar and turning upward and becoming nearly parallel to the jet in the vicinity of the jet boundary. Momentum is conserved. Momentum gained by the entrained water is equal to momentum lost by the jet. This causes the jet to slow down and broaden with height. Figure 5 shows the jet at the time it reaches the surface. The light flashes from the release pyrotechnics are approximately one diameter apart, so the broadening is apparent.

SURFACE INTERACTION, CROSS FLOW, AND BUOYANCY

Jet Broadening at the Surface and Cross Flow

There are actually two stages of broadening, the first being normal jet broadening due to turbulent mixing, and a second stage of much more rapid broadening immediately near the surface. Figure 13 shows the time averaged shape of the stagnation edge of air jets from a CCL in the water tunnel at Virginia Tech [6]. The cross flow is from right to left. Jet exit Mach numbers in the range of 0.28 to 1.9 are shown. For Mach numbers greater than 0.6 the jet stands up against the cross flow very well. The shape is the same for $.6 < M < 1.67$. Thus a vertical jet from a WPML has the same cross section as a golf tee, i.e. long and slender with a gradual increase of diameter and then a flaring out near the top. Photographs of the jet taken from above the surface are somewhat misleading in that they do not show the diameter of the jet at all, but the flared out diameter which is much larger. Also notice the exaggeration of the horizontal axis.

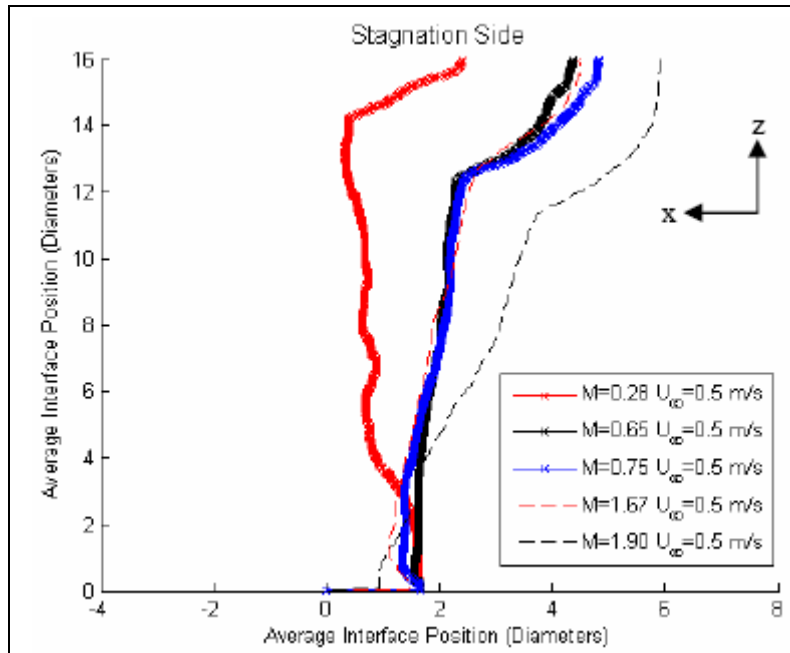


Figure 13. Time average interface position of an air jet in cross flow of .5 m/s (0.96 knot)

For the jets $0.6 < M < 1.67$ the spreading rate $db/dx = 0.186$ and the half angle is 10.5 degrees. This is a little broader than the tank test result at Blossom Point (7.4 degrees), but much narrower than rocket exhaust in air (13.7 degrees) and broader than water jets in water (6.8 degrees). For the $M = 1.67$ jet, the values are the same into cross flow as into still water. For jets with Mach numbers less than about .5, they “pinch off” shortly after reaching the surface and do not stand up very well against a cross flow.

Jet Buoyancy

As the jets slow, buoyancy becomes more important and the rate of mixing and spreading change accordingly. Momentum in the jet can be augmented by the buoyant forces and the jet can even be accelerated. For water jets in water the expansion rate is $0.105x$ in the buoyant region. The “momentum length” of a jet as obtained from dimensional analysis is the distance at which momentum gives way to buoyancy as the dominant mechanism. This has been amply confirmed for water jets in water, where jets inclined relative to vertical bend upward at this distance. The momentum length was used to nondimensionalize the jet trajectory data in Figure 7 above. For the JATO jet at 20 ft depth the momentum length is 240 ft, so buoyancy should not be important. There is no apparent buoyant effect in Figure 5. However, we have some data that show the distance for transition from momentum dominance to buoyancy dominance may be much less than the momentum length for rocket exhaust into water than water jets in water.

The trajectory for the jet tip from a MK-117 JATO motor fired at a depth of 42 ft. is shown in Figure 14. There is a pronounced change in speed at a height of 27 ft. at time 1.8 seconds. The exponent in the trajectory equation obtained from curve fitting shifts from 0.526 to 0.947. The momentum length is 190 ft. for the JATO at 42 ft. depth. From the figure it can be seen flow persists as a jet 0.45 seconds after motor burn out, and then becomes a buoyant plume. The scaled distance at the transition to buoyancy is 0.142 and the scaled time is 11.7. This point is at the upper cross on Figure 7.

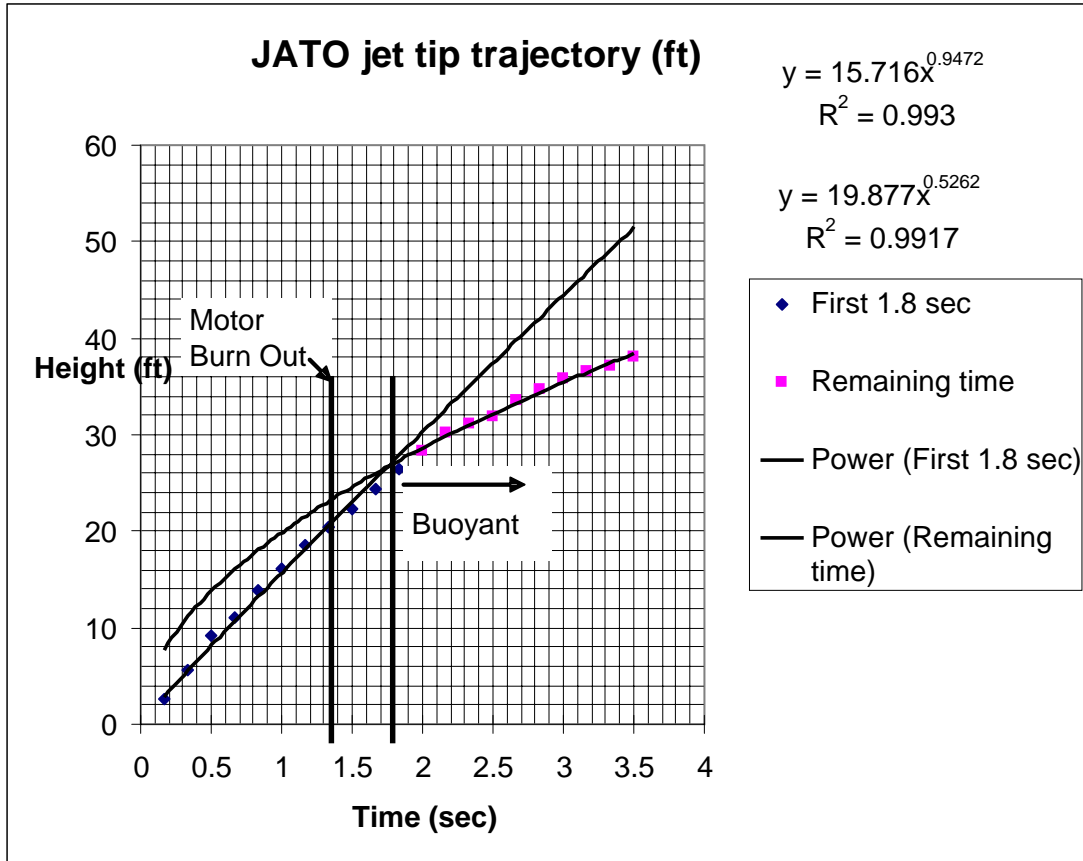


Figure 14. Jet Tip Trajectory For MK117 JATO Fired At A Depth Of 42 Ft.

We fired a SR-121 rocket motor at an inclination of 74.5 degrees to the horizontal (90 degrees is up) at a depth of 30ft. and found the jet turned upward at a distance of 11.5 ft. at time 1.28 seconds. Figure 15 shows the jet transition to a buoyant plume. When the jet got to the surface the time was 2.34 seconds and the knee in the trajectory curve was at 13.8 ft. The theoretical momentum length for this motor fired at 30 ft. is 339 ft. The scaled distance when the jet first turned upward was therefore 0.0339 and the scaled time was 6.79. This point is shown as the lower cross on Figure 7. When the jet arrived at the surface the knee was at a scaled

distance of 0.0407 and the scaled time was 12.45. Even though the momentum length for the SR-121 was greater than the MK-117 JATO, the transition to becoming a plume was closer to the launcher exit. Evidently momentum length is not a good predictor of the transition distance for gas jets in water.

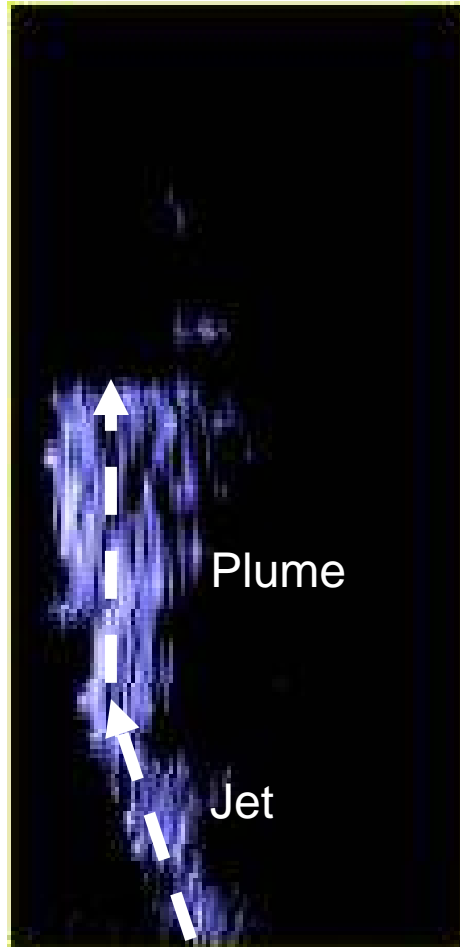


Figure 15. Inclined Jet From SR-121 Rocket Motor Transitioning To Become A Buoyant Plume.

JET INTERNAL STRUCTURE

Jet Cross Sectional Properties and Turbulence

The cross section through the jet at any given height shows nearly Gaussian distributions of the jet density, velocity and other properties. CFD results computed at NSWC are shown at the time the jet tip reaches the surface in Figures 16 and 17. The contours are for pressure and density, with embedded velocity profiles. The contours become Gaussian beyond the zone of flow establishment, which ends at 60 inches on the vertical axis. This distance is 6.6 equivalent diameters, which agrees with the zone of flow establishment ending at 6.2 diameters in Figure 9. For positions closer to the exit plane than 30 inches (3.3 equivalent diameters) the

velocity distribution is doughnut shaped. The approximately 7th power velocity distribution of internal flow in the annular space broadens, flattens, and becomes parabolic. At $x = 18$ (2 equivalent diameters) the parabolic distributions merge. The jet boundary angles from Figure 10, where $db(x)/dx$ is 0.26, are shown in Figure 17.

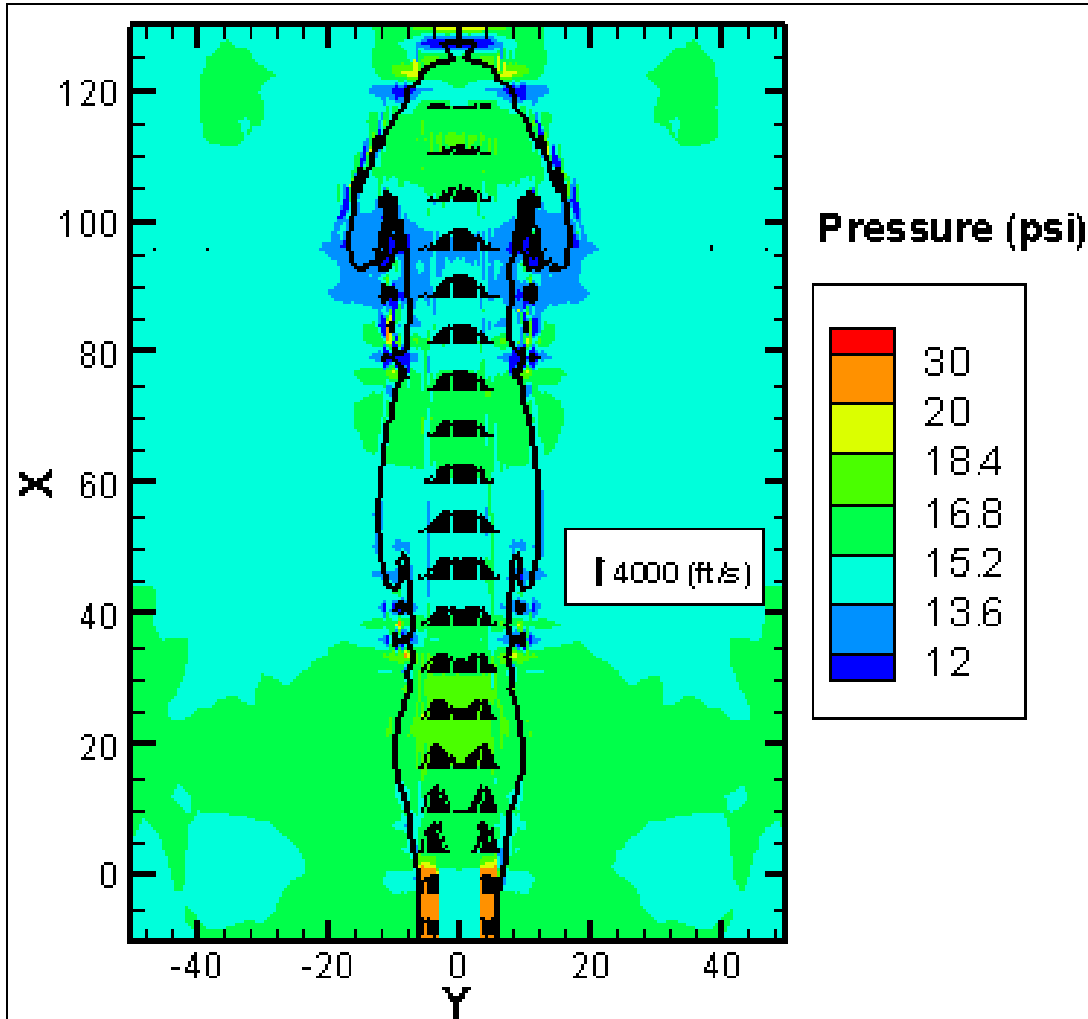


Figure 16. Pressure Contours For Jet. Length Scales Are In Inches.

The contours on Figure 17 show a sudden, near discontinuous change in density. The colors in the range 5 to 35 lb/ft³ are bunched into a solid line. The dark blue region is hot gas with some entrained water. The colors green through red are mainly water with some entrained gas. The computer results are in approximate agreement with the data of Loth and Faeth [5], even though the computer results are for a transient jet that has not reached steady state. The 0.5 air/water region which defines the jet diameter in [5] would be in the middle of the green region, which does not show on the plot because it is in the region of rapid change in the jet boundary.

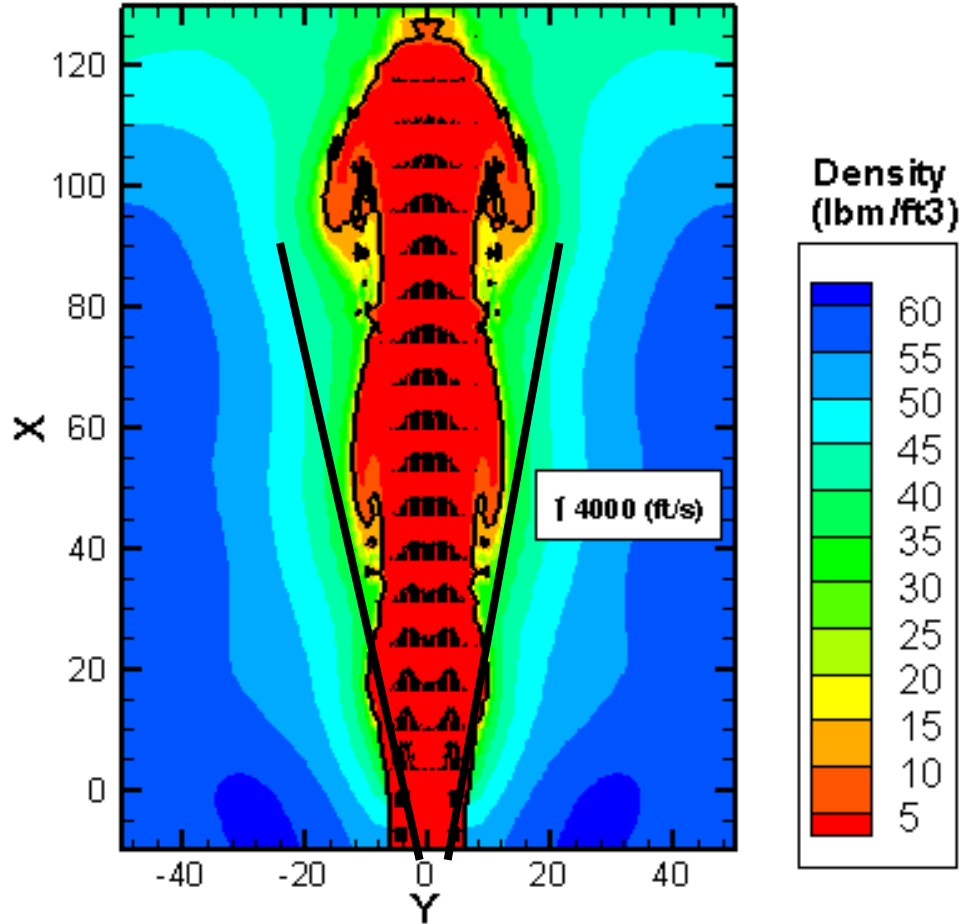


Figure 17. Density Contours For Jet. Length Scales Are In Inches. The Solid Lines Are From Figure 10, Where $B(X) = .26 X$.

Figure 18 (3.6 in [5]), shows a broad flat contour of turbulent rms intensities of 20-25% of the mean spanning the jet cross section. In the jet the fluctuations are most severe at the interface between the jet and the ambient, and the intensity profile shows two peaks. After the jet slows and becomes a plume, the shear at the interface between the jet and the ambient is less and the profiles show peak intensities along the centerline.

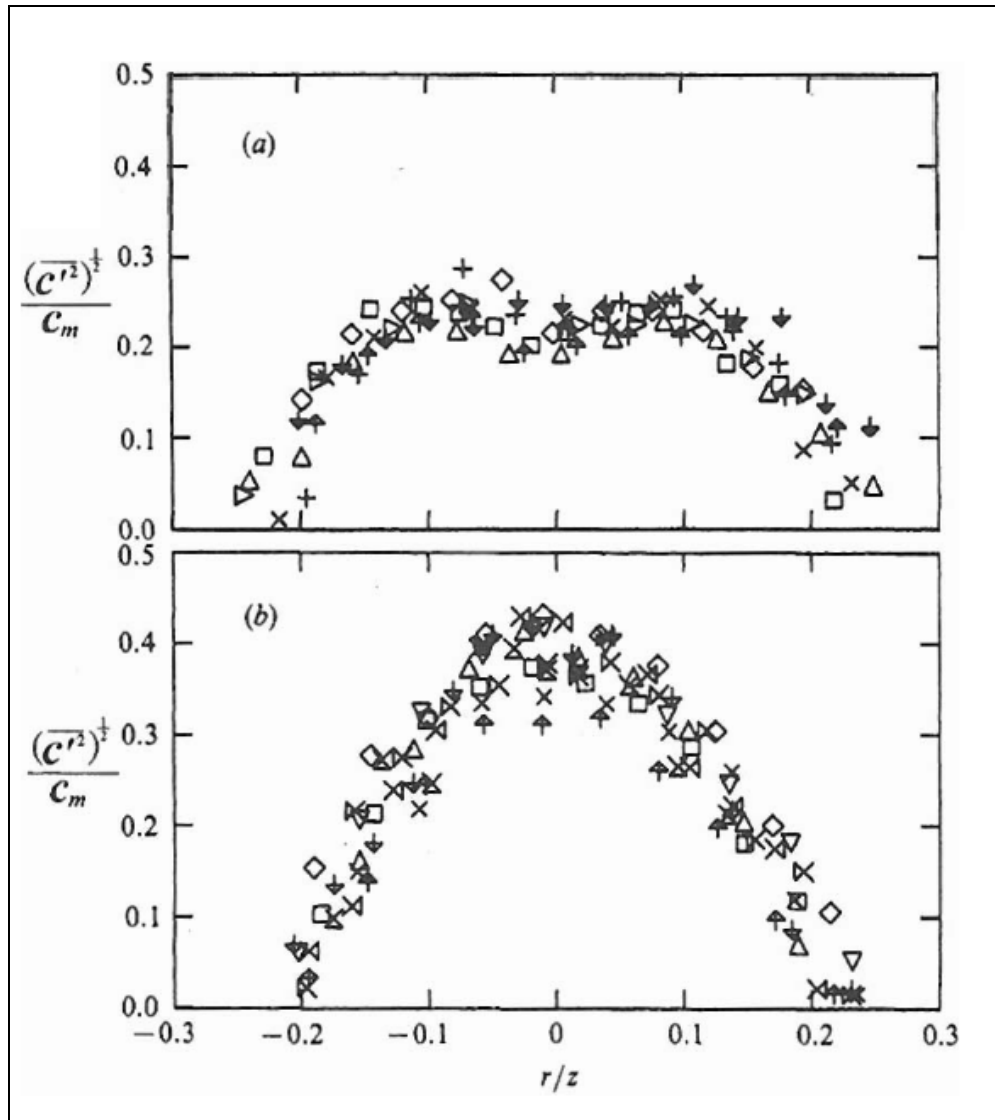


Figure 18. Turbulent Fluctuations Across A Jet (Top) And Plume (Below). The Fluctuations Are Rms Values.

The plots in Figures 16 and 17 show a jet with very high velocities in the core. Even though the core velocity is several thousand feet per second, the jet tip moves much slower. Differentiation of the trajectory equation on Figure 14 with respect to time yields a speed of 14.9 ft. per sec. over most of the burn time. The interface between the jet tip and water is Taylor unstable: a fluid trying to accelerate a second fluid of much higher density. The interface becomes highly irregular and turbulent. The high velocity gas core mixes with water at the jet tip and loses momentum very quickly in the mixing zone. This doesn't seem to cause much of a pressure disturbance in the mixing zone, but the density and velocity fields change very rapidly.

Approximate “low order” models of turbulent jets have been used extensively in civil and environmental engineering. Practically all the models are for steady flow. One example is the “top hat” model, which considers the properties to be uniform across the jet with the value being the average of the more accurate Gaussian distribution. For many problems in civil engineering the top hat model provides nearly the same result for broadening, mixing, and dilution as the Gaussian model, with much simplified calculations. The model used in our first try at the launch dynamics problem used a low order balloon filling model discussed above. It is a simple top hat model for nonsteady flow. As more data is obtained and the accuracy of CFD methods is confirmed, CFD will replace the low order semiempirical models.

SUMMARY

Turbulent rocket exhaust jets in water are similar in structure to water jets in water and gas jets in gas. Each case is characterized by a turbulent jet interface region that entrains the surrounding medium. The spreading rate db/dx and the half angle seems invariant with regard to scale and velocity, and unique to the phase of the medium and jet. They seem insensitive to the details of chemical composition. Methods for predicting the exhaust velocity and Mach number were discussed. Water depth is important, as increasing hydrostatic pressure decreases the exit Mach number and velocity. Gas jets can penetrate a considerable distance in water, and maintain a gas column out to at least 80 diameters. As the Mach number of gas jets in water approaches 0.6, the jet has the ability to penetrate a cross flow for a considerable distance. This makes the Water Piercing Missile Launcher plausible for moving platforms. Efforts are under way to develop low order semi-empirical models and computer fluid dynamics approaches to predicting detailed jet structures.

REFERENCES

1. J. Yagla, “Concentric Canister Launcher,” Naval Engineers Journal, May 1997, pages 313-330.
2. Yagla, Jon, Keith deLoach and Chris Weiland “The Water Piercing Missile Launcher,” 21st International Ballistics Symposium, Adelaide Australia
3. Fischer, H., List, J., Koh, R., Imberger, J., and Brooks, N. **Mixing in Inland and Coastal Waters**, Academic Press, New York, 1979.
4. Lee, J.H.W. and V.H. Chu **Turbulent Jets and Plumes**, Kluwer Academic Publishers, Norwell Massachusetts.
5. Loth, E. and G.M. Faeth “Structure of Underexpanded Round Air Jets Submerged in Water” International Journal of Multiphase Flow, Vol. 15, No. 4, pp 589-603, 1989.
6. Weiland, Chris, Jon J. Yagla, and Pavlos Vlachos “Experimental Study of the Stability of a High-Speed Gas Jet Under the Influence of Liquid Cross-Flow” Proceedings of FEDSM2007 5th Joint ASME/JSME Fluids Engineering

Conference, July 30-August 2, 2007 San Diego, CA.